A Comprehensive Study of the Ionospheric Response to Two Intense Geomagnetic Storms of Solar Cycle 24 over Asian and American Region: A Comparative Analysis

Dur-e-Shahwar Kamran[2], Usman Tahir[1], Muhammad Mudassar Abasi[2]

[1]Department of Physics, University of Wah, Wah Cantt 47040, Pakistan.

Keywords

Geomagnetic storm, Ionospheric irregularities, Solar activity, Ionospheric VTEC variation, St Patrik day storm,

Abstract

Geomagnetic storms are space weather events that greatly impact the earth's magnetosphere and ionosphere, causing disturbances in satellite communication, navigation systems, and ground-based power grids. This study investigates the ionospheric irregularities in response to two intense geomagnetic storms (march 2015 and June 2015) of solar cycle 24 over two longitudinal sectors. In order to analyze the ionospheric response, sound analysis of solar wind parameters (of the above-mentioned events) and total electron content (TEC) variations (via line as well as contour plots) is presented. The results show significant seasonal diurnal as well as regional TEC variations, indicating distinct response to solar wind parameters, specifically the interplanetary magnetic field Bz component, which are highly correlated with the storm's intensity. During both events significant TEC enhancement can be seen during the early hours of the storms, which vary longitudinally. The findings of this study can be used to improve space weather modeling and prediction, ultimately helping mitigate the adverse effects of space weather on technological systems.

1 Introduction

The study of ionospheric behavior during a geomagnetic storm is essential in space weather forecasting and in high frequency radio communication. The disturbance in earth magnetosphere cause by solar activity such as coronal mass ejection (CME, S) is term as geomagnetic storm. During a geomagnetic storm energy and momentum carried by solar wind is transmitted into the magnetosphere, ionosphere and thermosphere. This led to the complex ionospheric structures including electric field and current system. These factors disturb the ionospheric composition specifically total electron content (TEC) causing ionospheric storm. The increase in TEC is called positive ionospheric storm were as the decrease is referred to as negative storm. Positive ionospheric storm is most likely driven by the interplay of various factor such as auroral particle precipitation, equatorward neutral wind, penetration and disturbance dynamo electric field etc, and are usually short-lived (K. K. Hashimoto, 2020). The eastward penetration field causes upward plasma drift which in term move plasma along the magnetic field lines toward higher latitude, where the molecular recombination rate is slow. Due to the upward plasma drift, TEC increases in topside ionosphere. On the other side negative ionospheric storm are mostly associated with the changes in neutral composition, the propagation of electron density trough from high to low latitude and the fountain effect. Ionosphere plays a crucial role in radiocommunication as it reflects and refract radio waves align them to cover longer distances. Geomagnetic storm can impact the radio communication as they disrupt the ionosphere electron density, that causes signal absorption and scattering. These storms alter the radio wave propagation path leading to signal delays and losses. This effect can damage satellite communication, Navigation system and astronaut's physical health. Understanding the role of ionosphere and effects of geomagnetic storms is important for mitigating and ensuring reliable radio communication system. The variation in ionosphere which result due to changes in magnetosphere, usually called the ionospheric storm is a complex phenomenon which is not fully understood up till know. There are multiple drivers of ionospheric storm due to which the predication of these storms is very difficult, therefore for in depth analysis of ionospheric behavior during geomagnetic storm, the parameter namely vertical total electron content (VTEC) plays a critical role. VTEC data can be obtain from global navigation satellite system (GNSS). By using VTEC we can analyze the ionospheric irregularities at different latitudes and altitudes. Also, the regional and hemispheric differences can be highlighted through VTEC. This study aims to investigate the VTEC variation over the two longitudinal sectors (Asia and America) for the St Patrik day storm and 22-23 June 2015 geomagnetic storm to provide new insights in the understanding of geomagnetic storms based on regional, Diurnal and seasonal effects.

2 Data sets and Methodology

Measurements from ACE satellite, ground-based GNSS receivers and from the Swarm constellation make up the observational portion of our work. The data of solar wind parameter is taken from the ACE satellite which is available at OMNI WEB. The region where the magnetic field of earth is dominant is known as magnetosphere. When the charged particle from the solar wind gets trapped into the earth magnetosphere, they are only allowed to move in specific trajectories the current that is generated due to the movement of these charge particle is known as ring current. The intensity of geomagnetic storm depends on the magnitude of ring currents. In order to analyze the storm strength, we will used global geomagnetic SYM/H index having resolution of 1 mint. By using data from the network of magnetometer around the world we can calculate SYM/H (al. E. E., 2005).

Based on the SYM/H (al. N. P., 2013) we can categories the geomagnetic storm as

Category	Geomagnetic Storm Intensity
Minor Storm	≥−30
Moderate storm	-50 to -30
Serve storm	-100 to -50

Super storm	250 to -100

Table 1 Classification of Geomagnetic storms on the basis of SHYM/H values

The total number of electrons which are present per meter cross section from the earth surface to the top of ionosphere is known as total electron content. The TEC is an important parameter that is not only used to describe the level of ionization in the ionosphere but it is also used in radio wave propagation for the calibration of single frequency GPS and satellite communication. During the geomagnetic storm the value of the TEC increase and decrease and it will effect the propagation of signal through the ionosphere. The straight ray path which a signal follows from satellite to the GPS receiver is called Slant TEC while only its vertical component is called VTEC. The vertical total electron content (VTEC) can be computed using data from GPS receivers.

2.1.1 GPS derived vertical total electron content calculation

When the GPS signal travel form satellite to ground base GPS receiver the ionosphere that is the conductive medium disturb the propagation of the signal. The free electron that is present in the atmosphere cause the phase shift and delay in the signal. The refractive index of ionosphere varies with altitude and given by Appleton-Hatree equation, which can be written in simplified form as

$$n^* = (1 - \frac{f_p^2}{f^2})^{1/2} \approx (1 - \frac{f_p^2}{2f^2})$$

$$n^* = 1 - \frac{40.3n}{f^2}$$

Where

$$f_p = \frac{ne^2}{8\pi \in_0 m_e}$$

is electron-plasma frequency in Hz and n is number density in m − 3. The expression for the phase velocity is

$$v_p = \frac{w}{k} = \frac{c}{n^*} = c\ (1 - \frac{40.3n}{f^2})^{-1} \approx (1 + \frac{40.3n}{f^2})$$

where c is the speed of light. As we know that the carrier wave has no information until it is modulated, and the modulated wave travels with group velocity which is always less than c. The expression of group velocity is

$$v_g = \frac{\partial w}{\partial k} = \frac{c}{n^*} = c\,(1 + \frac{40.3n}{f^2})^{-1} \approx c(1 - \frac{40.3n}{f^2})$$

As the refractive index depends on electron density and wave frequency this shows that speed of waves varies along their path in the ionosphere (al, 2001). The duration required for a signal to propagate in the ionosphere is determined by

$$\tau_g = \int \frac{ds}{v_g} = \frac{1}{c}\int (1 + \frac{40.3n}{f^2})\,ds \approx \tau_0 \frac{40.3}{f^2}\int nds$$

Where τ_g denotes time taken by wave in the case of vacuum and s is the path of wave. The total number of electrons in the 1m2 column along the signal's passage is denoted by $\int$ nds. This is measured in TECU units and is referred to as slant total electron content (TEC) where

$$\text{TECU} = \frac{10^{16}e}{m^2}$$

When the GPS signal travel form the ionosphere that is the conductive medium it will disturb the propagation of the signal (as discussed above). Distinct refractive indexes are provided for modulated and carrier waves, respectively, by

$$n_p = 1 + \frac{40.3N}{f^2}$$

And

$$n_p = 1 - \frac{40.3N}{f^2}$$

Where N is the electron density measured in electrons/m3 and f denotes frequency measured in Hz. The electromagnetic distance between satellite and GPS receiver can be find by

$$s = \int_{sat}^{rec} nds$$

For the carrier wave this distance is given by

$$s_c = \int_{sat}^{rec} 1 + \frac{40.3N}{f^2} ds$$

$$s_c = \int_{sat}^{rec} ds \ + \frac{40.3}{f^2}\int_{sat}^{rec} Nds$$

where the linear distance between the GPS receiver and satellite is $\int_{sat}^{rec} ds = r$. So, we can write as

$$s_c = r + \frac{40.3}{f^2}(TEC)$$

The electromagnetic distance for modulated wave is similarly

$$s_m = r - \frac{40.3}{f^2}(TEC)$$

Ionospheric delay is the term for the error caused on by the signal's passage through the ionosphere. It is given by

$$d_{tono} = \frac{40.3}{f^2}(TEC)$$

Where f is the frequency of the GPS signal that is known so the ionospheric delay is just only function of TEC. The final expression for calculating the value of TEC is

$$TEC = \frac{1}{40.3}\left(\frac{f_1 f_2}{f_1^2 - f_2^2}\right)(p_2 - p_1)$$

This expression is called as slant total electron content (Marković, 2014).
The connection between the vertical total electron content and the slant total electron content is

$$VTEC = STEC.COZ\ (Z)$$

Finally, VTEC can be computed from STEC by using the above relation (al. T. Y., 2014).

3. Results and Discussion

This section presents the underlying causes of two distinct geomagnetic storms, as well as an analysis of the geomagnetic indices and the Analyze solar wind parameter. We examine the ionospheric parameter VTEC simultaneously, which was collected from four ionosonde stations from America and Asia.

3.1 Solar wind parameters for St Patrick day storm

Solar and geomagnetic variations are important factors that affects the ionospheric density resulting in ionospheric irregularities during a storm. So, the data of solar wind parameters such as speed (km/s), pressure (nPa), interplanetary magnetic field (Bz in nT) and the geomagnetic index SYM/H (nT)provided by the omni web link is analyzed. The first largest geomagnetic storm of solar cycle 24 was initiated from a C9.1/1F flare erupted on 15 March 2015 which reached the Earth on 17 March 2015. The solar wind and geomagnetic indices were quiet before 17 March as shown in figure. On 17 March at about 4:30 UT. Figure 3.1shows the variation in solar wind parameter during the initial phase (IP), main phase (MP) and recovery phase (RP) of the storm. First panel indicates the intense fluctuation in Bz component on the day of storm. During the early hours of storm Bz turns northward indicating the sudden storm commencement (SSC) (Wilcox, 1968). As the MP begin Bz turn southward and during this period pressure and speed of solar wind rises abruptly. The corresponding SYM/H index varies directly with Bz. As Bz turn southward SYM/H start decreasing and reaches its minimum value -234nT at about 22UT as seen in the 4th panel. Based on SYM/H observation National Oceanic and Atmospheric Administration (NOAA) classified this storm as G4 category geomagnetic storm.

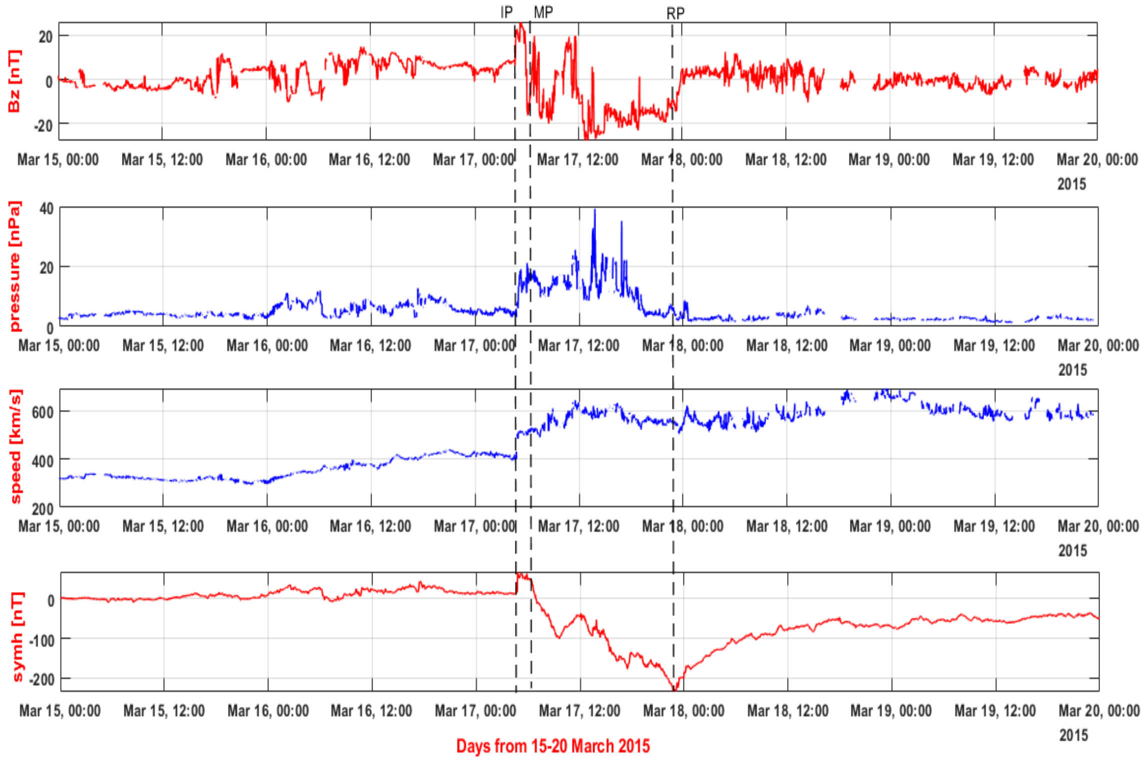

Figure 1 Global parameters (from top to bottom) of geomagnetic storm for 15-20

3.2 Ionospheric TEC variation over the Asian/American sector for St Patrick day storm

To estimate the VTEC maps the dual frequency observation of about four GNSS station provided by UNAVCO are used for VTEC plots of both regions. Figure illustrate the VTEC maps of Asian and American sectors. The vertical bar shows the value of VTEC in TECU. It can be seen that before the onset of the storm, ionospheric VTEC kept at low level. In the MP it enhances significantly to about 120 TECU at 16:45 UT over American region and at 12 UT over Asian region. After the MP notable decrease in VTEC can be observed indicating negative storm more prominent over Asian region. However, the positive storm effect where dominant over American region.

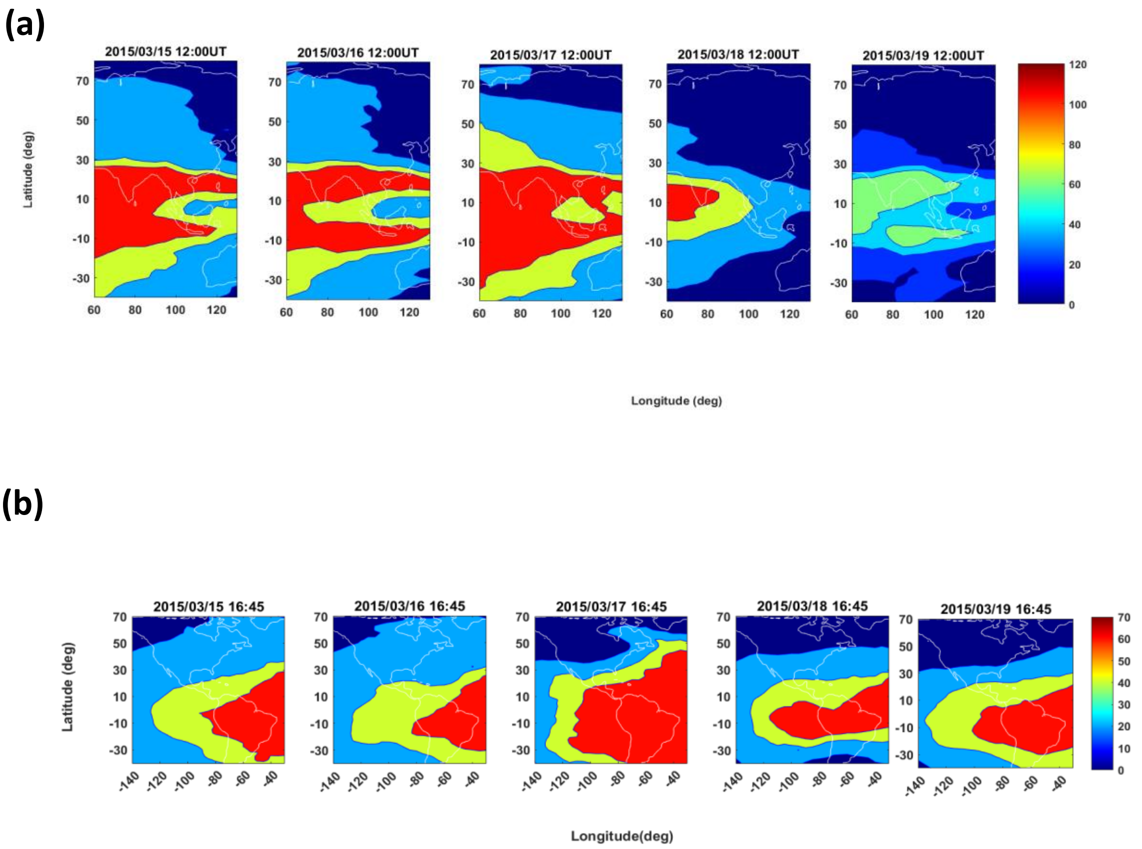

Figure 2 VTEC contour map from 15-19 for Asian and American region of 17 March 2015

The above result can be verified using line plots. The VTEC line plot is a significant tool. It represents remarkable variation in both space and time depending on longitude, latitude. Universal time, season and solar cycle. Also, the intensity of geomagnetic storm can be analyzed using VTEC values.

Figure shows the VTEC over two longitudinal sector that are under study. Universal time is taken along horizontal axis while the vertical axis represents the increase or decrease in VTEC. Inside each panel two super imposed line curve can be seen. The line curve with blue color indicates quiet time values of VTEC and red color show VTEC variation during the storm. From the graph it is noticed that VTEC enhancement occurred during local noon in America, this is because on the day of the storm, America is at the dayside while Asia is at night side. Also, both regions exhibit VTEC enhancement at low and mid latitudes but double peaks are observed in American region exhibiting positive storm effect. However, more negative storm effects are observed in Asian region during the recovery phase of the storm. These observations are well consistent with the above contour plots.

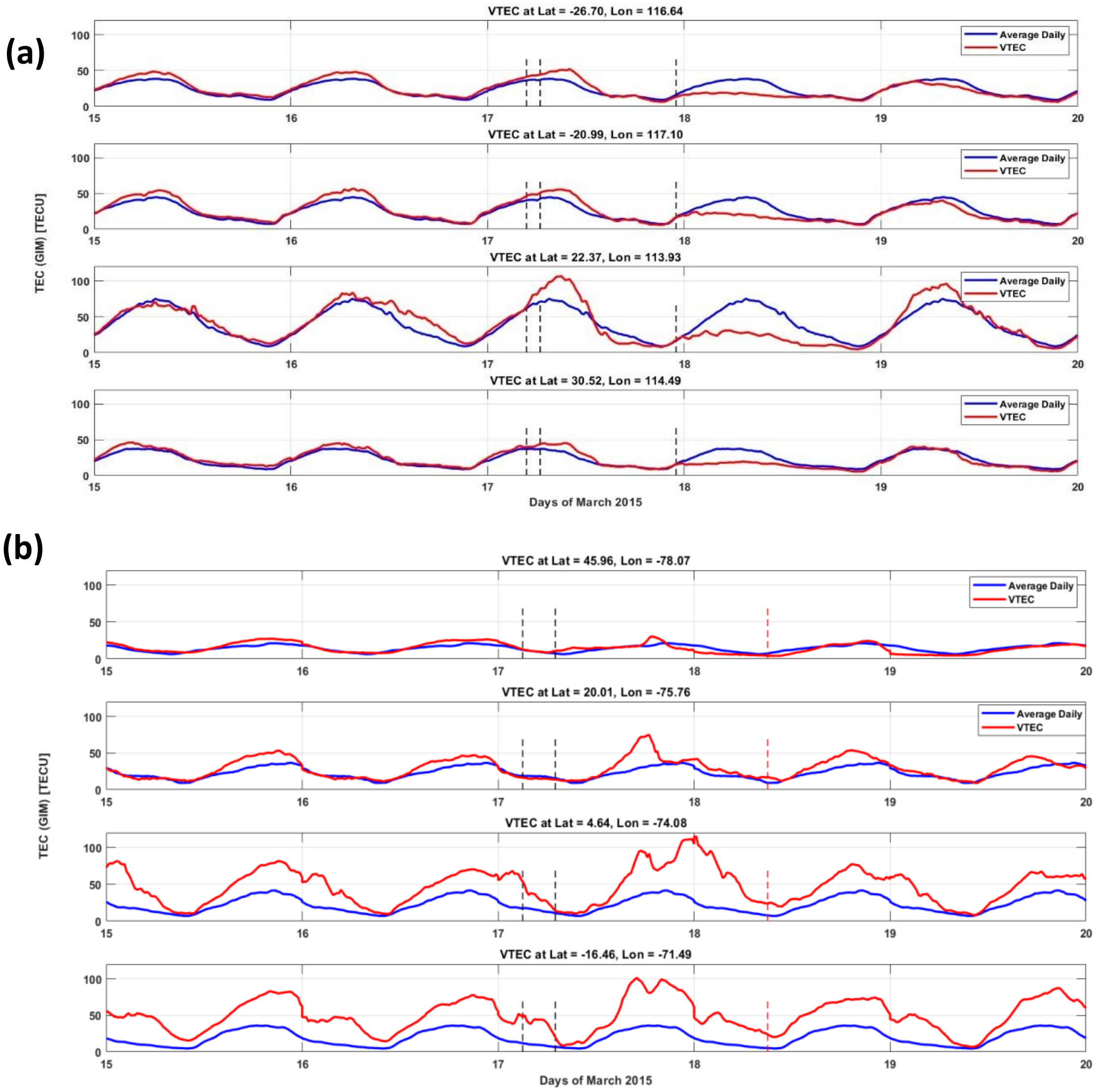

Figure 3 a) VTEC line map from 15-19 for Asian region of 17 March 2015. b) VTEC line map from 15-19 for American region of 17 March 2015

3.3 Solar wind parameters for June 2015 storm

The second largest geomagnetic storm associated with three CMEs. The first one arrived at earth on 21 June 2015, second at early hours of 22 June 2015while third and largest one reach earth at late hours on 22 June 2015 at about 18:30 UT. This was the Halo CME which is the main cause of the storm. The Bz component of IMF at initial phase is southward as shown in Figure. The velocity of solar wind is recorded highly variable 450-700 km/s. The corresponding SYM/H index increases upto 70 nT for a very short period of time and then decreases to a minimum value of -207 nT. During this event the MP lasted early as compared to St Patrick day storm. Also, the solar wind response is less intense than the opposite case

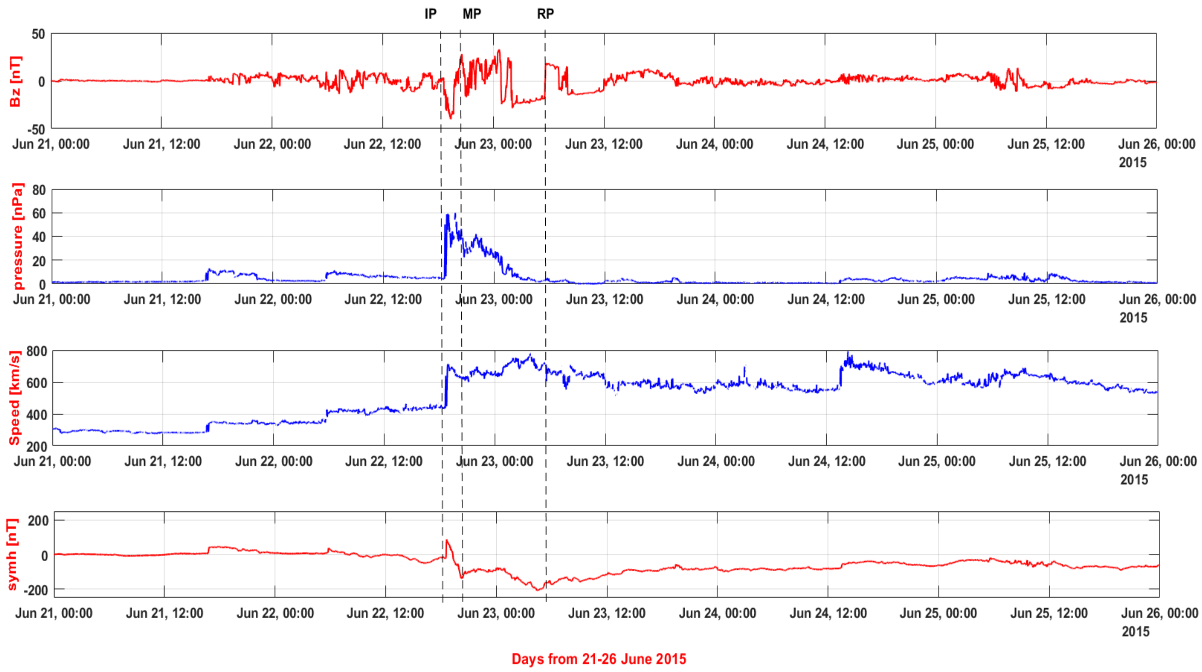

Figure 4 Global parameters (from top to bottom) of geomagnetic storm for 21-26

3.4 Ionospheric TEC variation over the Asian/American sector for June 2015 storm

If we look at the Figure same kind of observation are observed as during March 2015 storm on the basis of latitude but there is a large decrease in VTEC. Although the origin of this storm is related to more intense flare but the effect is less intense as compared to March 2015 storm. The effects are first observed over American region on 22 June 2015 at about 23 UT. However geomagnetic storm effect over Asian sector is observed on 23 June 2015. Also, more strong negative effects are seen over American region during this event. The VTEC line plots for June 2015 geomagnetic storm over America and Asian sector is dissipated using Figure. From the figure it can be visualized that positive storm effect occur at low latitude but are comparatively less than St Patrik day storm time variations. In addition, a significant negative storm is observed during the recovery phase in our region of interest. However, the duration and onset of main and recovery phase is different in both regions.

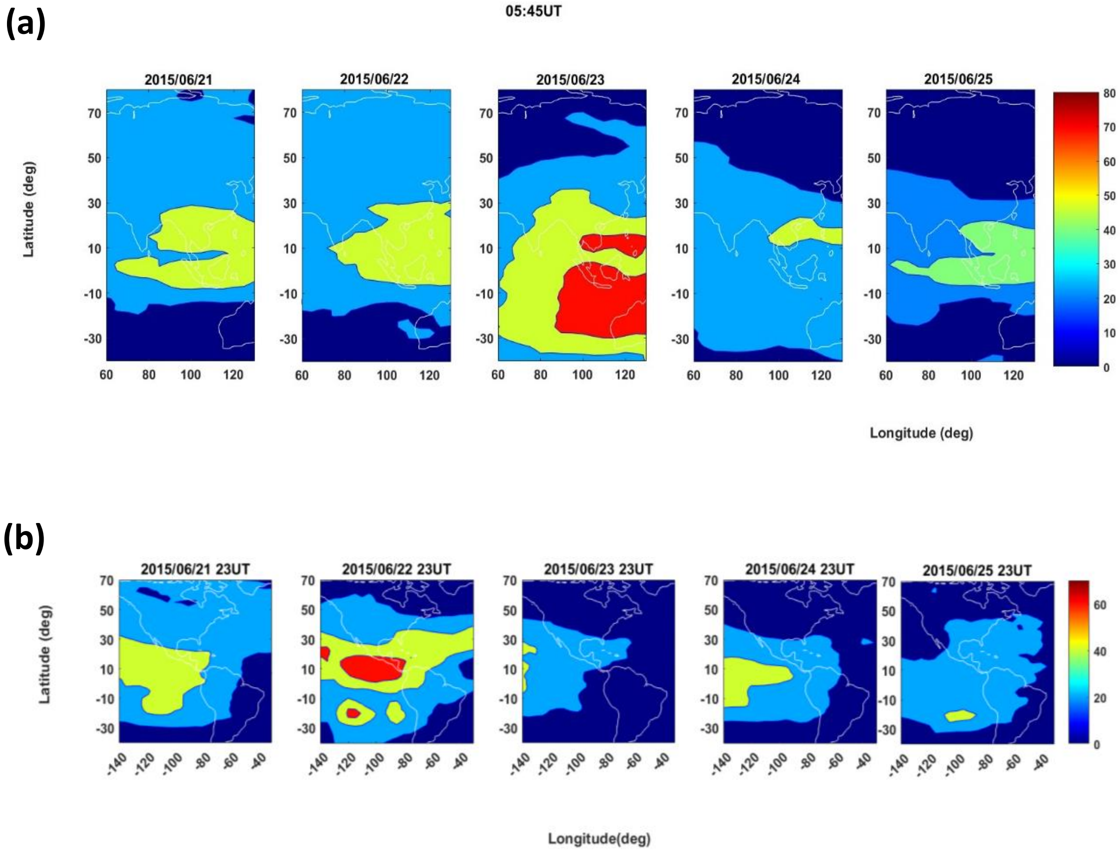

Figure 5 VTEC contour map from 21-26 for Asian and American region of 22 June 2015

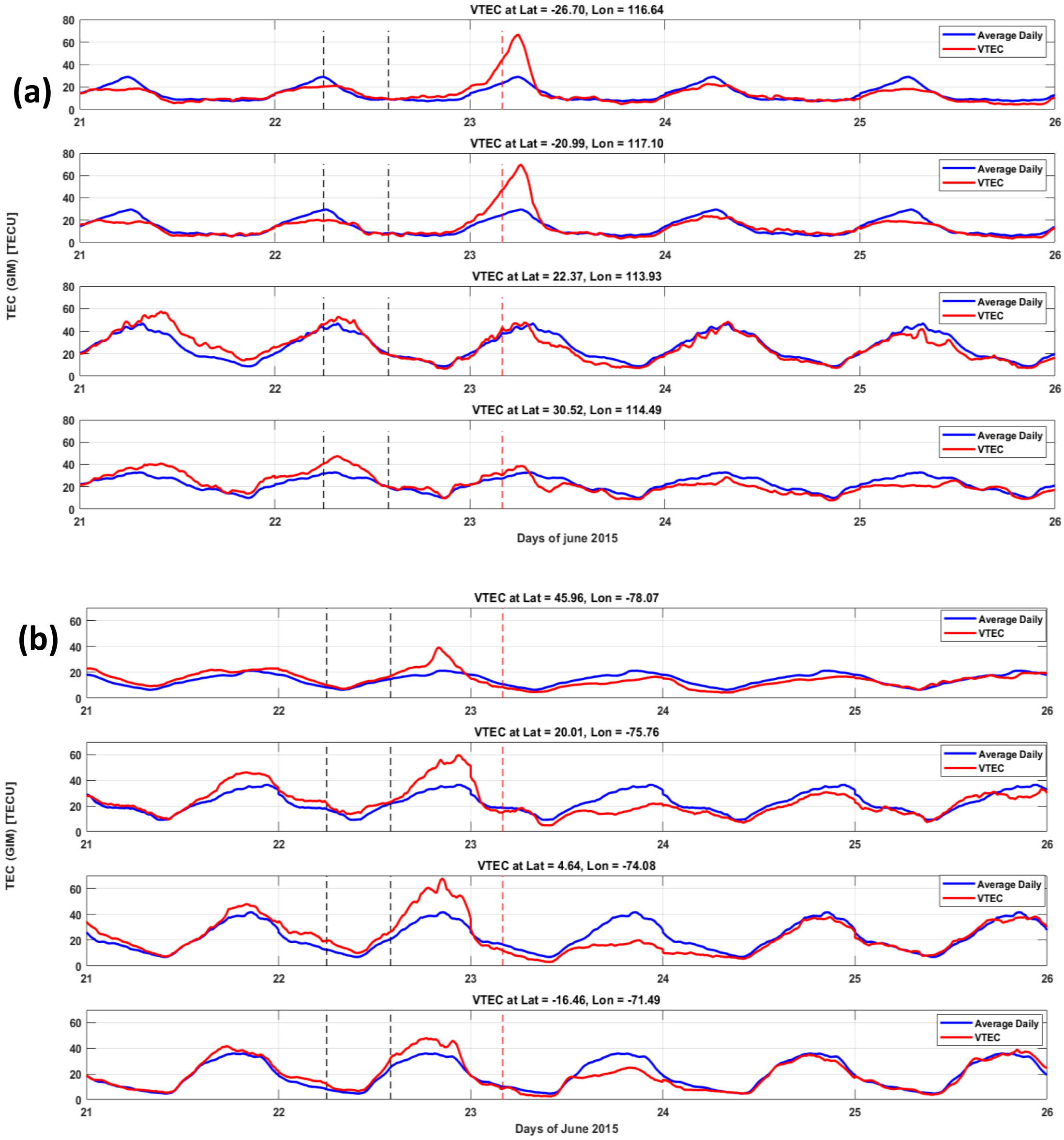

Figure 6 VTEC line map from 21-26 for Asian region of 22 June 2015. b) VTEC line map from 21-26 for American region of 22 June 2

3.5 Possible physical mechanism

The purpose of this study is to investigate the geomagnetic storm effect in opposite season equinox and summer solstice.

The comparative study of the geomagnetic storm on 17 March 2015 and 22-23 June 2015 reveals distinct differences in their impact on the earth magnetic field and upper atmosphere. The March 2015 storm triggered by a coronal mass ejection (CME) exhibit a more intense and rapid increase in geomagnetic activity, resulting in a stronger disturbances of the earth magnetic field. In contrast the June 2015 storm commenced by a high-speed solar wind stream showed a more gradual and prolonged increase in geomagnetic activity leading to more sustained disturbance. The TEC variation during the two storm also different significantly. The result shows that the geomagnetic storm varied considerably between the American and Asian sector. The march 2015 storm exhibited a more pounced impact on Asian sector with enhanced TEC and geomagnetic disturbance whereas the American sector experienced the storm positive peaks on the day of storm for a short time. This is due to longitude and time. The Asian region is more susceptible to solar wind energy input due to its proximity to the dawn to dusk meridian. Also, the storms peak activity occurred during Asian night time when the ionosphere is more sensitive to the solar wind disturbances. Another factor which contributed to this difference is the solar wind speed which is 550-600 km/s for Asian sector and 450-50 km/s for American sector. These factors combine to produce the observed differences in VTEC values between both regions during 17 March 2015 geomagnetic storm.

During June 2015 geomagnetic storm VTEC variation are prominent at low latitudes particularly near equator in Asian region and at low and mid latitude in American region but theses variation is less intense as compare to march event (al. E. A., 2017). This is because of difference in season and hemisphere. The variations in VTEC for both cases arise due to different energy input as the first event occurred during equinox whereas, the second event took place in solstice season.

The latitudinal variations in VTEC arise due to the combine effect of two dynamos i.e. magnetospheric disturbance dynamo and ionospheric disturbance dynamo (Richmond, 1980). Magnetospheric disturbance dynamo give rise to prompt penetration electric fields (PPEFs) due to particle precipitation. Positive storms occur due to the influence of these PPEFs usually during the main phase of the storm (al. B. N., 2016). However, these fields are short lived as they transfer their energy to ionosphere due to magnetosphere-ionosphere coupling. In response, Ionospheric disturbance dynamo arise which in turn generates disturbed dynamo electric fields (DDEFs) (B. G. Fejer, 2017) . These are comparatively long lived and are responsible for negative storm at the end of main phase and during the recovery phase. Mainly the magnetospheric dynamo arise due to solar wind-magnetosphere coupling while ionospheric dynamo occurs due to magnetosphere-ionosphere-thermosphere coupling.

As we are familiar well with the fact that during solar wind-magnetosphere interactions, energy transfer occurs. Auroral region is mainly the site where coupling of interplanetary magnetic field (IMF), magnetosphere, ionosphere and thermosphere take place. Here the precipitation of particles causes the ionosphere conductivities to increase. As a result, field aligned currents (FACs) are produced that connects magnetosphere to ionosphere. During the day, the ionization of ionosphere increases due to solar radiations leading to the generation of electric fields. As a result of interaction of these electric fields with magnetic field generates eastward equatorial electrojets. The direction of flow of these currents are eastward at magnetic equator. The conductivities of ionosphere are different in direction. Pederson conductivities are parallel to electric field and perpendicular to magnetic field. On the other hand, Hall conductivities are perpendicular to electric field as well as magnetic field (Maute, 2020). These conductivities give rise to Pederson and Hall currents. Pederson current follows path parallel to the electric field. Hall currents propagate perpendicular to both electric field and magnetic field. These currents move plasma through the ionosphere and thermosphere. This plasma movement drags the neutrals in thermosphere through transfer of momentum by Ampere's law that produces joule heating which in turn give rise to Thermospheric winds which are responsible for diurnal variations. This whole process of generation and flow of currents and winds is called the disturbance dynamo. The energy input for this overall process depends upon certain factors such as seasons (al. W. Y., 2022), solar activity, the location of a region from where the variations are being observed with respect to Sun (dayside or nightside).

4. Conclusion

In our work we use data from various sources and performed the comparative analysis and understood the physics behind the two cases. The finding of both these cases point to the importance of season and storm onset timing in determining the impact of storm. Therefore, we shall consider all the factors in order to fully analyze the impact of the geomagnetic storm.

- Less intense solar flare can also cause major geomagnetic storm.
- SYM/H index categorized both event as G4 geomagnetic storm.
- Ionosphere response differently in dayside and nightside sector.
- Positive storm occurs in main phase while negative storm occurs in recovery phase.
- The different duration of initial and main phase also contributes in VTEC variation.
- Seasonal effects play major role in overall differences observed.

References

al, N. J. (2001). Space Weather Effects in the Ionosphere and Their Impact on Positioning. ESA Workshop Paper.

al., B. N. (2016). Middle- and Low-Latitude Ionosphere Response to 2015 St. Patrick's Day Geomagnetic Storm. Journal of Geophysical Research: Space Physics, 3421–3438.

al., E. A. (2017). Global Ionospheric and Thermospheric Effects of the June 2015 Geomagnetic Disturbances: Multi-Instrumental Observations and Modeling. Journal of Geophysical Research: Space Physics, 11,716–11,735.

al., E. E. (2005). Introduction to Space Weather. Advances in Space Research, 855–865.

al., N. P. (2013). Statistical Properties of Substorms During Different Storm and Solar Cycle Phases. Annales Geophysicae, 349–358.

al., T. Y. (2014). Simulation Study on Slant-to-Vertical Deviation in Two Dimensional TEC Mapping Over the Ionosphere Equatorial Anomaly. Advances in Space Research, 595–603.
al., W. Y. (2022). Ionospheric Response to the Coronal Hole Activity of August 2020: A Global Multi-Instrumental Overview. Space Weather.
B. G. Fejer, M. B. (2017). Post-Storm Middle and Low-Latitude Ionospheric Electric Fields Effects. Space Science Reviews, 407–429.
K. K. Hashimoto, T. K. (2020). Penetration Electric Fields Observed at Middle and Low Latitudes During the 22 June 2015 Geomagnetic Storm. Earth, Planets and Space, 1-15.
Marković, M. (2014). Determination of Total Electron Content in the Ionosphere Using GPS Technology. Geonauka, 1-9.
Maute, R. A. (2020). Challenges to Understanding the Earth's Ionosphere and Thermosphere. Journal of Geophysical Research: Space Physics.
Richmond, M. B. (1980). The Ionospheric Disturbance Dynamo. Journal of Geophysical Research: Space Physics, 1669–1686.
Wilcox, J. M. (1968). The Interplanetary Magnetic Field: Solar Origin and Terrestrial Effects. Space Science Reviews, 258–328.

…………….

List of Tables

Table 1: Categorization of geomagnetic storm on the basis of SYM/H index.

Figures Captions

Figure 1:: Global parameters (from top to bottom) of geomagnetic storm for 15-20 March 2015. Vertical dotted lines correspond to Initial, main and recovery phase of the geomagnetic storm.

Figure 2: **a)** VTEC contour map from 15-19 for Asian and American region of 17 March 2015

Figure 3: **a)** VTEC line map from 15-19 for Asian region of 17 March 2015. **b)** VTEC line map from 15-19 for American region of 17 March 2015

Figure 4: Global parameters (from top to bottom) of geomagnetic storm for 21-26 June 2015.

Figure 5: VTEC contour map from 21-26 for Asian and American region of 22 June 2015

Figure 6: a) VTEC line map from 21-26 for Asian region of 22 June 2015. **b)** VTEC line map from 21-26 for American region of 22 June 2